

Technical Report

TR-23-19

October 2023



Creep of Cu-OFP in presence of sulphides

Tiina Ikäläinen

Timo Saario

Zaiqing Que

SVENSK KÄRNBRÄNSLEHANTERING AB

SWEDISH NUCLEAR FUEL
AND WASTE MANAGEMENT CO

Box 3091, SE-169 03 Solna
Phone +46 8 459 84 00
skb.se

SVENSK KÄRNBRÄNSLEHANTERING

ISSN 1404-0344

SKB TR-23-19

ID 2011458

October 2023

Creep of Cu-OFP in presence of sulphides

Tiina Ikäläinen, Timo Saario, Zaiqing Que

VTT

This report concerns a study which was conducted for Svensk Kärnbränslehantering AB (SKB). The conclusions and viewpoints presented in the report are those of the authors. SKB may draw modified conclusions, based on additional literature sources and/or expert opinions.

This report is published on www.skb.se

© 2023 Svensk Kärnbränslehantering AB

Summary

The first part of the study involved testing of two Cu-OFP tensile specimens (of the design used further on in this study for creep investigations) in air at room temperature. Microscopy revealed a number of micro-crack type defects on the surface of the tested specimens.

Cu-OFP creep specimens were exposed to sulphide containing pH = 7.2 water at T = 25 °C, at a stress level of 135 MPa. Removal of the sulphide from water by N₂ bubbling resulted in a dramatic and very rapid transient increase in strain rate, by about two orders of magnitude, the transient lasting for about 20 hrs. Influence of the sulphide exposure on the hydrogen concentration in the Cu-OFP material was studied by stopping one test, removing the creep specimen from the autoclave as fast as possible (within 23 min) and placing it in liquid nitrogen before having the hydrogen concentration measured. The sulphide exposure was found to markedly increase the hydrogen content within Cu-OFP material.

A rather detailed SEM-study was performed on both the creep specimens and coupon specimens exposed at the same time as the creep specimens. Based on the work, the following conclusions were made:

- hydrogen does enter Cu-OFP during exposure to sulphide containing water,
- the increase in Cu-OFP creep rate caused by removal of sulphide from the water occurs at such a high rate, that the mechanism is most likely that of hydrogen in the Cu-OFP moving out and causing excessive dislocation movement,
- dynamic creep deformation influences the morphology of the surface film forming on Cu-OFP; instead of the typical double-layer surface film, a single layer of nano-crystalline film is formed,
- straining of Cu-OFP tensile specimens (to the fracture strain of about 25 %, much higher than the strain achieved in the creep tests) causes micro-cracks to appear on the surface, originating from pre-existing defects.

Contents

1	Introduction	7
2	Goal	9
3	Description	11
4	Methods	13
5	Results	15
5.1	Air tests	15
5.2	Tests in sulphide containing water	18
5.2.1	Sulphide test 1	18
5.2.2	Sulphide test 2	21
5.3	HME and SEM studies	24
5.3.1	Hydrogen measurement	24
5.3.2	SEM studies of the coupon samples	24
5.3.3	SEM studies of the creep specimens	28
5.3.4	Compilation of data from SEM studies	32
6	Discussion and Conclusions	33
	References	35

1 Introduction

In previous work for SKB with Cu-OFP base material (Ikäläinen et al. 2022) VTT has found that when the sulphide feed into the test vessel (autoclave) was stopped, the creep rate of Cu-OFP, after a few hours increased more than one order of magnitude. However, the effect was transient and the creep rate returned to the level before stopping the sulphide feed within a few tens of hours. Two different mechanisms for the phenomena were suggested.

The first one involves the possibility that hydrogen enters Cu-OFP during exposure (the HS^- reacts with Cu producing a Cu_xS -surface film and the H^+ -ion diffuses into the Cu-base metal) and as the HS^- is removed from the solution, hydrogen mobility in the base metal increases and causes additional plastic deformation. In order to have an effect on the strain rate (i.e. affect the dislocation structures) hydrogen need not leave the sample but move within the material. During the exposure, after reaching the steady-state of corrosion (film formation at the film/metal interface and film dissolution at the film/solution interface occur at equal rate), there is a dynamic equilibrium of hydrogen concentration in the material and HS^- concentration in the water phase. When HS^- concentration in the water phase decreases, the dynamic equilibrium shifts causing hydrogen movement (and re-arrangement of the dislocation structure) to start within the material. In this mechanism, the creep rate returns to a stable level when the hydrogen concentration in the base material reaches a new equilibrium.

The second mechanism involves reductive dissolution of the Cu_xS -surface film as a result of decreasing “sulphide pressure” on the water side. In this mechanism, the reductive dissolution produces vacancies within the base material, which again facilitates dislocation movement and increases the creep rate. Also in this mechanism, the creep rate returns to its original level when the surface film has reached a new equilibrium with the water and the vacancy concentration in the base material also reaches a new equilibrium.

The work in this project aims at defining the prevailing mechanism causing the transient increase in creep rate.

2 Goal

The aim of the work was to determine which mechanism is responsible for the transient acceleration of the creep rate of Cu-OFP when sulphide feed is stopped.

3 Description

The Cu-OFP material studied was delivered by SKB. The received material had approximate dimensions of $170 \times 130 \times 50$ mm, cut from the tube T58. The material had been characterised and found to meet the post-production requirements. The average mechanical properties of nine samples representing different locations within the tube material are shown in Table 3-1. The average concentration of phosphorous and impurities is shown in Table 3-2.

Table 3-1. Average room temperature mechanical properties of the material (Välimäki 2009).

R_{p0.2} N/mm²	R_m N/mm²	Elongation %	Hardness HV5
42	212	52	43

Table 3-2. The average phosphorous and impurity concentration of the material, in wt-ppm (Välimäki 2009).

P ppm	S ppm	O ppm	H ppm
58.7	5.4	3.0	0.43

4 Methods

The Cu-OFP specimens had dimensions of 0.5 mm (thickness), 8 mm (width) and 29 mm (length of the deforming part of the body). The specimen design is shown in Figure 4-1. The specimens were manufactured using electric discharge machining (EDM). Possible increase in hydrogen concentration of the Cu-OFP due to the EDM would have plenty of time to diffuse out, since the specimens were used only after several weeks or even months from manufacturing. Before testing, the deforming part of the specimen body was polished (#220, #500 and #1200 SiC-papers successively) to remove the EDM-affected surface layer. Thus, the actual specimen thickness was about 0.4 mm.

The specimens were attached to the loading grips of a tensile machine, electrically insulated from the grips by ZrO_2 parts. The loading part was attached to an autoclave lid and placed inside the autoclave body. All autoclave parts were made of AISI 316L stainless steel. The pull rod extended through the autoclave lid via a Ballseal™ spring loaded sealing element, with a friction force of 59 N at room temperature. The autoclave was equipped with a $Ag/AgCl(0.05\text{ M KCl})$ reference electrode and a Pt counter electrode. An Autolab PGSTAT302F potentiostat with Nova 2.0 software was used to measure the potential of the specimen, no external applied current or potential was used. The loading of the specimen was controlled by Cormet SSRT system v. 4.03.

Tests performed in sulphide containing water the experiments were performed in a stainless steel autoclave in a phosphate buffer ($Na_2HPO_4 \cdot 2H_2O / NaH_2PO_4 \cdot 2H_2O$) solution of $pH = 7.2$. The sulphide addition ($Na_2S \cdot H_2O$, 60–63 %) was made at a target concentration of 32 mg/l (1 mM) to a 10 l glass stock vessel filled with the buffer solution, which was previously bubbled oxygen free with 5N N_2 -gas (Aga Ltd). After adding the sulphide, the autoclave was bubbled oxygen free with 5N N_2 -gas and a tube pump (Cole-Parmer Instrument Co.) was used to pump the electrolyte through the autoclave. After flowing through the autoclave, the solution was directed to a 40 l storage tank where $FeCl_3 \cdot 6H_2O$ was used to neutralize sulphide. The pH at the end of the experiment was measured at about $pH = 7.3$.

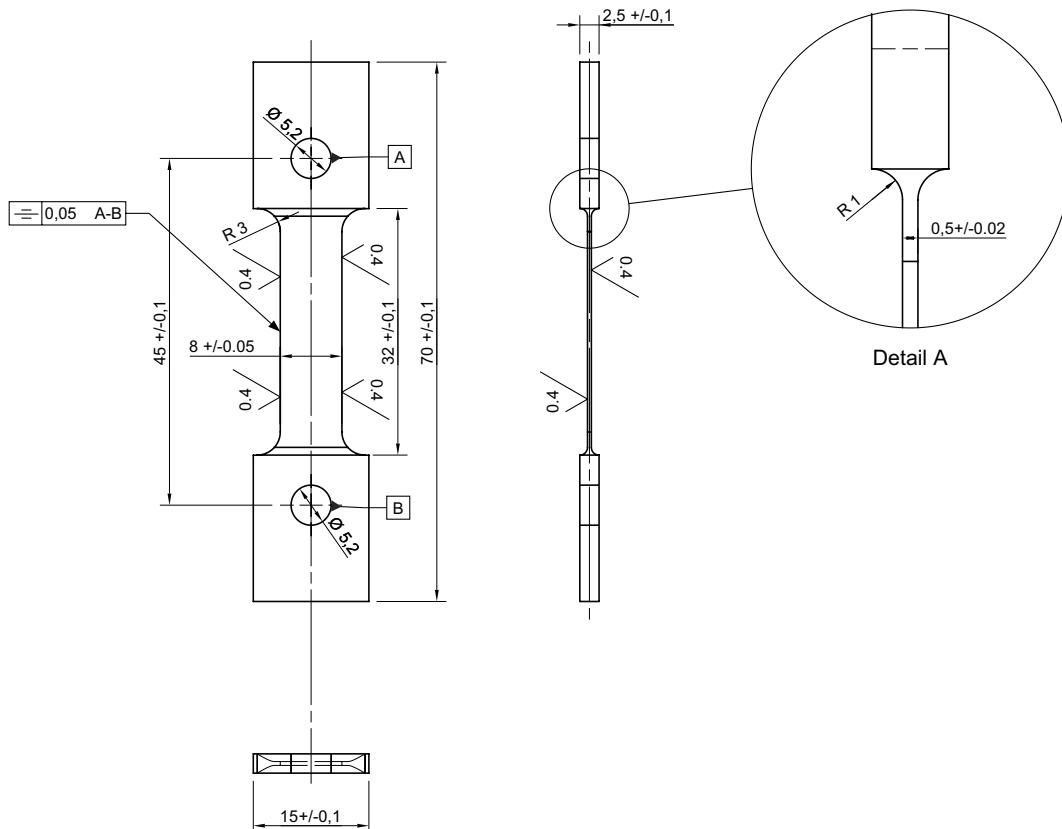


Figure 4-1. Specimen design.

The sulphide concentration was measured from the autoclave outlet from grab samples using Chemetrics C-9510D-kit for large concentrations (5 to 300 mg/L).

The glass stock vessel was pressurized to 0.5 bar overpressure with 5N N₂ to keep oxygen out and to balance the pressure drop caused by the outgoing flow. At the pH used in this experiment, about 45 % of the sulphide is in the form of gaseous H₂S, Figure 4-2. Since no continuous bubbling through was used (only pressurization) gaseous H₂S was not able to escape from the stock solution and the sulphide in the stock solution tended to stay constant.

Hydrogen concentration was measured with Hot Melt Extraction (HME)-technique using Bruker G8 ON/H MS device and thermal conduction detector (TCD).

With regard the scanning electron microscopy (SEM) studies, a field emission gun – scanning electron microscope (FEG-SEM) Zeiss Crossbeam 540 equipped with solid-state four-quadrant backscatter detector was used to characterize specimens.

The specimen surface and cross sections were analysed by SEM-secondary electron (SE) imaging and backscatter electron (BSE) imaging. SE imaging was performed at a working distance (WD) of 10–15 mm with 15–20 keV, 1.5–3 nA. BSE images were acquired with the solid-state four-quadrant backscatter detector at 15–20 keV acceleration voltage with WD of 5–7 mm. Film layer chemical analysis was performed with SEM-Energy Dispersive X-Ray (EDX) with 20 keV, 3 nA. SE mode is more sensitive to surface layer topography. BSE are based on the dependence of the backscatter electron signal on the orientation of crystal lattice planes with respect to incident electron beam due to electron channeling, thus is more sensitive on crystal structure and chemical composition.

The specimen outer surface from each specimen was checked with SE and EDX spot analysis. The cross-sectional film from each specimen was checked with SE and BSE and EDX area mapping.

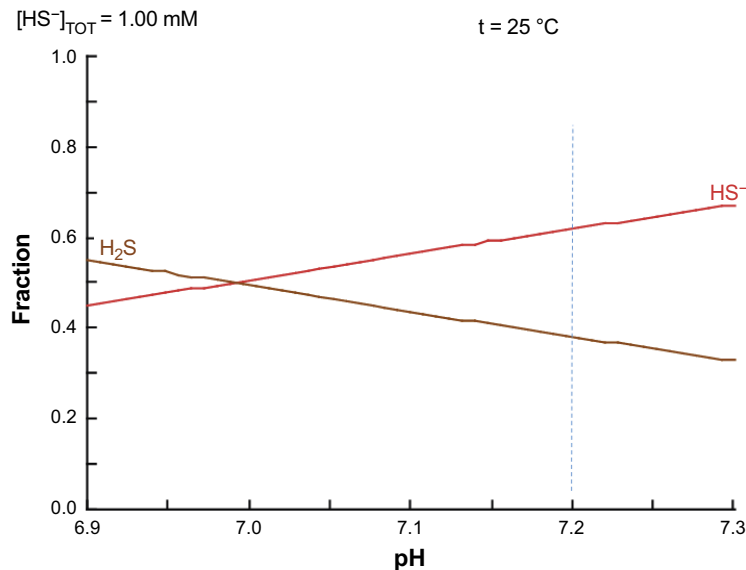


Figure 4-2. Equilibrium speciation of H₂S/HS⁻ as a function of pH. The dotted blue line depicts the pH in the current experiment (Lilja 2021).

5 Results

5.1 Air tests

Two specimens were first tested in air to find out the stress-strain behaviour of the material. The strain rate used was $\dot{\epsilon} = 3 \times 10^{-5} \text{ s}^{-1}$. The specimens were photographed before testing, see Figure 5-1. The stress-strain curves are shown in Figure 5-2. The yield stress was about 65 MPa, clearly higher than that reported in Table 3-1 for the material. This is most likely due to the cold deformation produced by the polishing operation. For such a thin specimen, the deformed layer may form a large part of the thickness. The fracture strain was markedly lower, 27 % for specimen Air 1 and 22 % for specimen Air 2, than that reported for the material (42 %, see Table 3-1). Both specimens showed many micro-crack like features after the test, Figure 5-3 and Figure 5-4. Although not a planned part of this study, the surface of the specimen Air 2 was studied with SEM. As evidenced by Figure 5-5, the features are indeed micro-cracks, the length of which is in the range of a few tens of μm .

The main purpose in the air tests was to measure the stress-strain curve of Cu-OFP for the specimen design used in this study, to establish a solid ground for selecting the stress level for the further tests in sulphide containing water. Since the results show that the fracture strain for this specimen design is markedly lower than what was expected based on the material data shown in Table 3-1, and to maintain direct comparability with earlier results in sulphide containing water, it was decided to perform the sulphide tests at the same stress level as before, i.e. 135 MPa. Since the gauge thickness of the samples is only about 0.45 mm (after removing the EDM affected layer), the cold deformation introduced in polishing reaches through a substantial part of the cross-section. Therefore, the material is in partially cold deformed state after the polishing. Thus, the measured fracture strain falls clearly below the level normal to annealed material.

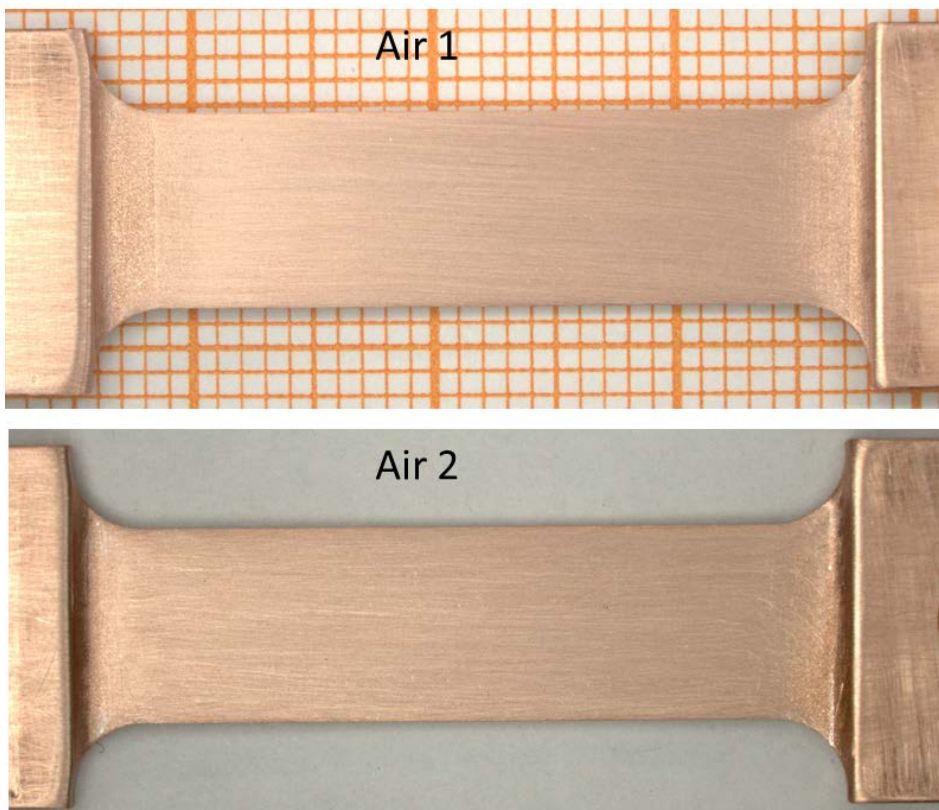


Figure 5-1. Air test specimens after polishing (before testing).

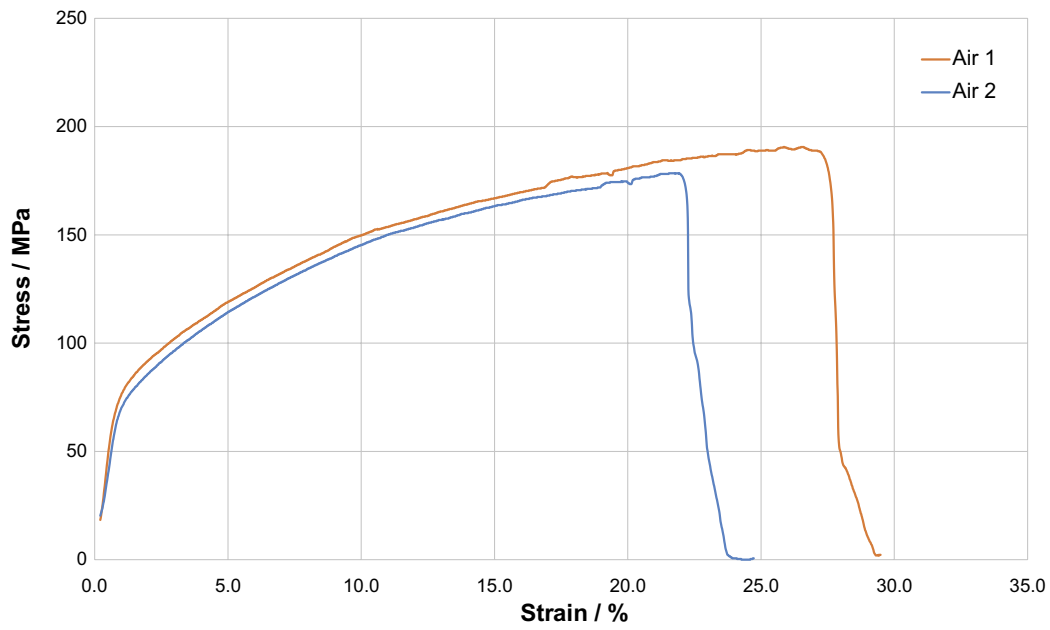


Figure 5-2. Stress-strain curves of Cu-OFP in air.

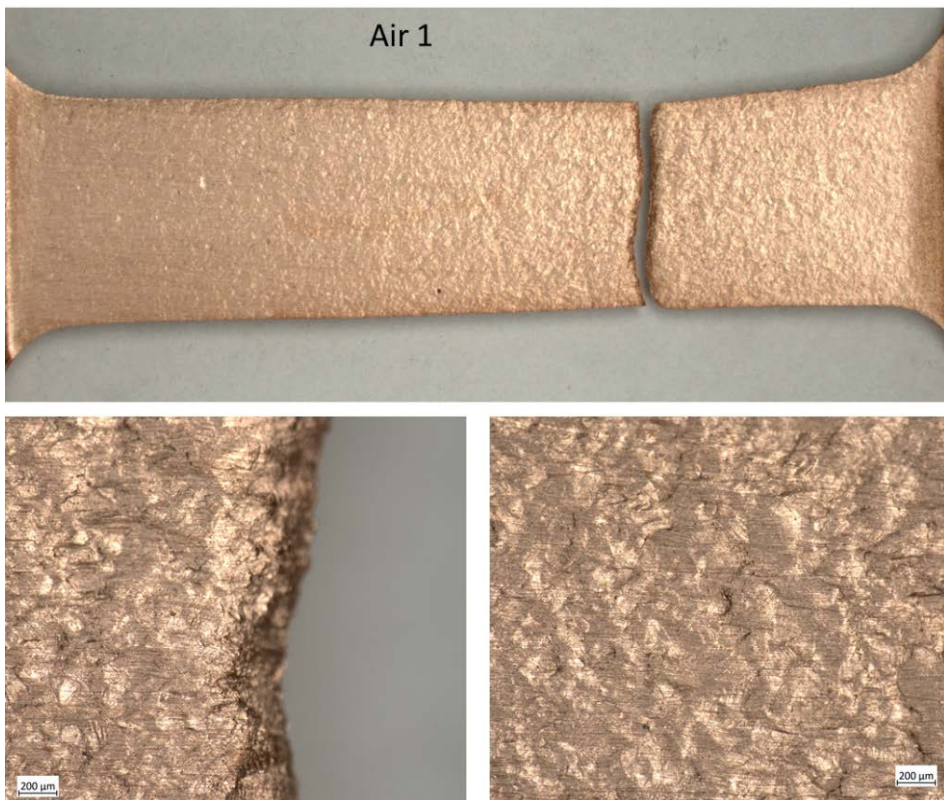


Figure 5-3. Surface appearance of specimen Air 1 after the test.

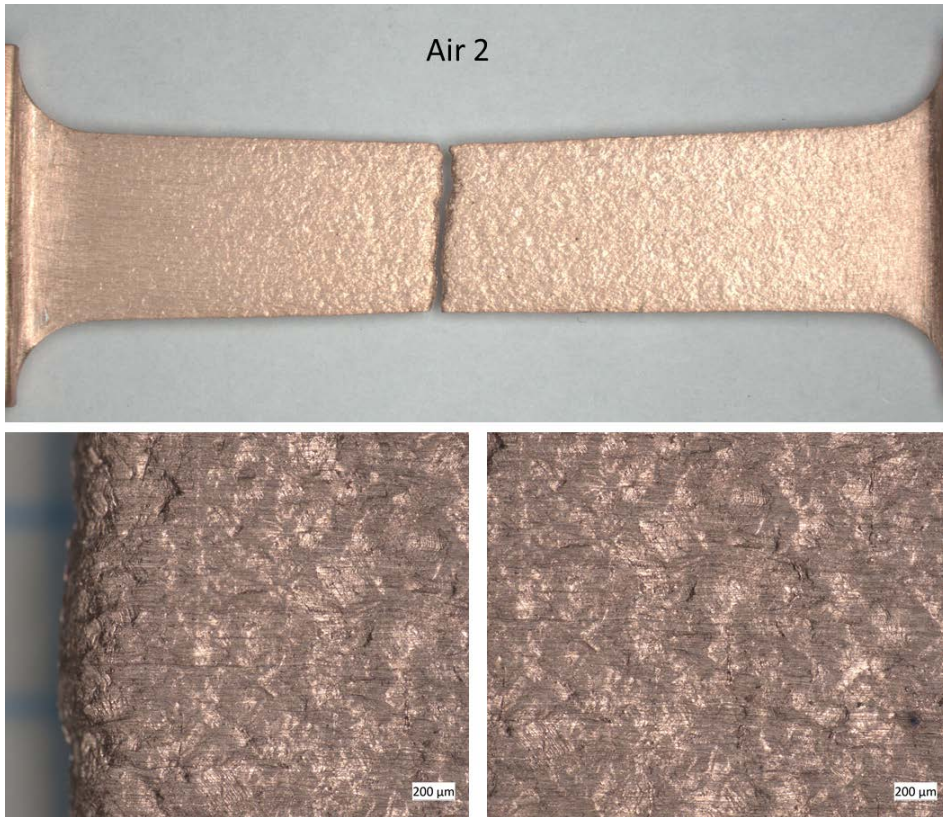


Figure 5-4. Surface appearance of specimen Air 2 after the test.

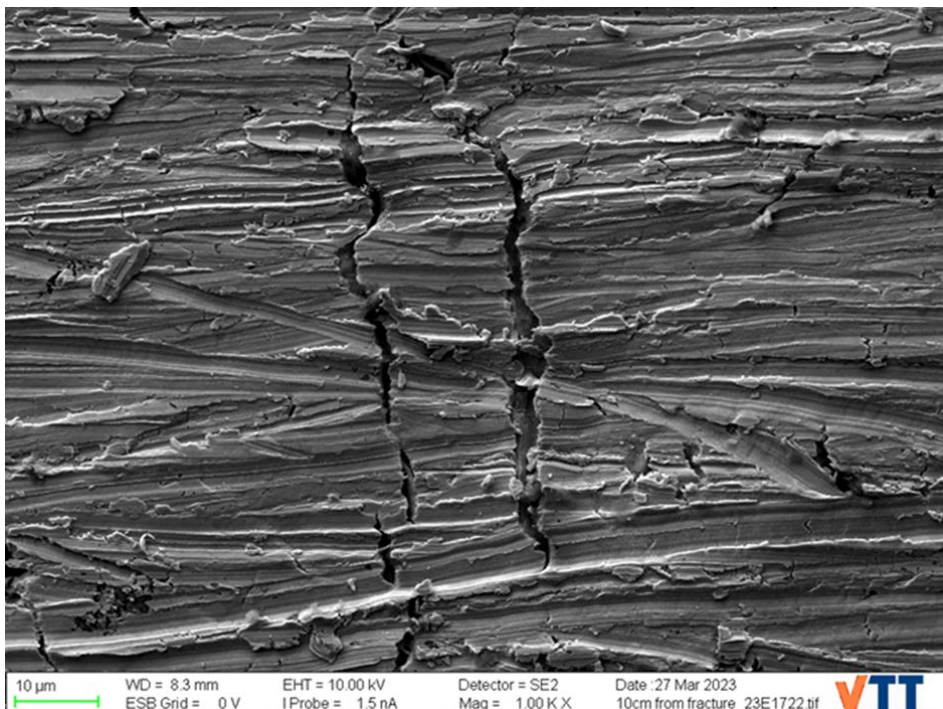


Figure 5-5. SEM-picture of one micro-crack found on the surface of specimen Air 2 (located about 1 cm away from the main fracture surface). Here the loading direction is horizontal.

5.2 Tests in sulphide containing water

Two creep tests were performed in sulphide containing water at the stress level of 135 MPa. Loading was only performed after it was established that the sulphide concentration at the autoclave outlet was at the target concentration of 32 mg/l (within the measurement accuracy). Loading was started at $t = 0.8$ hrs for sulphide test 1 and at $t = 4.1$ hrs for sulphide test 2.

5.2.1 Sulphide test 1

The corrosion potential of the sample is shown as a function of exposure time in Figure 5-6. Also the sulphide measurement results are shown in the figure at appropriate times, and indicate that during the sulphide feed the sulphide concentration stayed at the targeted level. The sulphide feed was stopped at $t = 48$ hrs. At about $t = 67$ hrs, bubbling was started with 5N N_2 -gas to remove the H_2S in the autoclave gas phase and thus expedite the removal of sulphide from the water phase as well. At this point, the corrosion potential started to increase, indicating decreasing of the sulphide concentration in the water. In our experience, the corrosion potential, during transient conditions in the electrolyte, is typically dominated by the existing surface film. For a thick film (like in this case), it may take quite a while to adjust to the changes in the environment. Based on this, we would not expect to see a direct, in-time, dependency of the corrosion potential measured and the HS^- concentration in the electrolyte.

The stress and elongation during the first test are shown in Figure 5-7 as a function of time. Also the sulphide measurement results are shown in the figure at appropriate times. The corrosion potential and strain rate are shown in Figure 5-8 as a function of time. After stopping the sulphide feed at $t = 48$ hrs, no acceleration of elongation rate (creep rate) was observed for the next about 19 hrs. The sulphide concentration measured at this point (at about $t = 67$ hrs) showed that the concentration was still at the same level, i.e. 30 mg/l, as during the sulphide feed. At about $t = 67$ hrs, bubbling was started with 5N N_2 -gas to remove the sulphide in the autoclave water phase. An immediate rapid increase in both the elongation and strain rate was observed, Figure 5-7 and Figure 5-8. During the first 30 minutes the elongation increased by 76.7 μm , corresponding to an additional strain of about 0.26 %.

During the sulphide feed, the system was at atmospheric pressure (due to the outlet line being open to the discharge vessel). However, when the N_2 bubbling was initiated, an overpressure of 0.5 bar was applied, resulting in an increase in the loading of about 4 N, causing an increase in the stress level by about 1 MPa (to 136 MPa). In order to find out the effect of the increase of the stress level on the creep behaviour, an increase of the load by 4 N was deliberately made at about $t = 138$ hrs (i.e. after the creep rate had stabilized after the increase due to the start of the N_2 bubbling and accompanied pressure increase). As seen in Figure 5-7 the increase of the load by 4 N resulted in a transient increase in elongation and strain rates, albeit much smaller than in the case of the initiation of the N_2 bubbling. In this case, during the first 30 min, the elongation increased by 0.29 μm , corresponding to an additional strain of about 0.001 %.

This result indicates that the increase of elongation rate (and creep rate), as a consequence of starting the bubbling with 5N N_2 -gas to remove the H_2S in the gas phase (at about $t = 67$ hrs) was caused dominantly by another reason than the increase by 4 N in the pure mechanical loading.

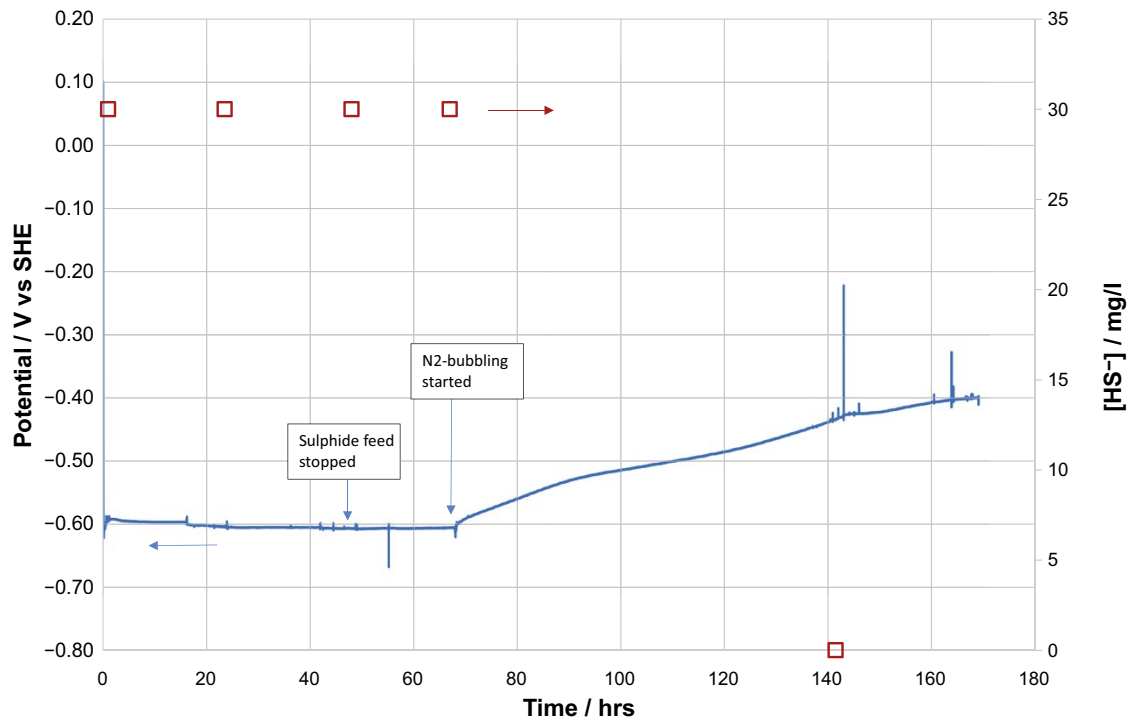


Figure 5-6. The corrosion potential and sulphide concentration as a function of time for sulphide test 1.

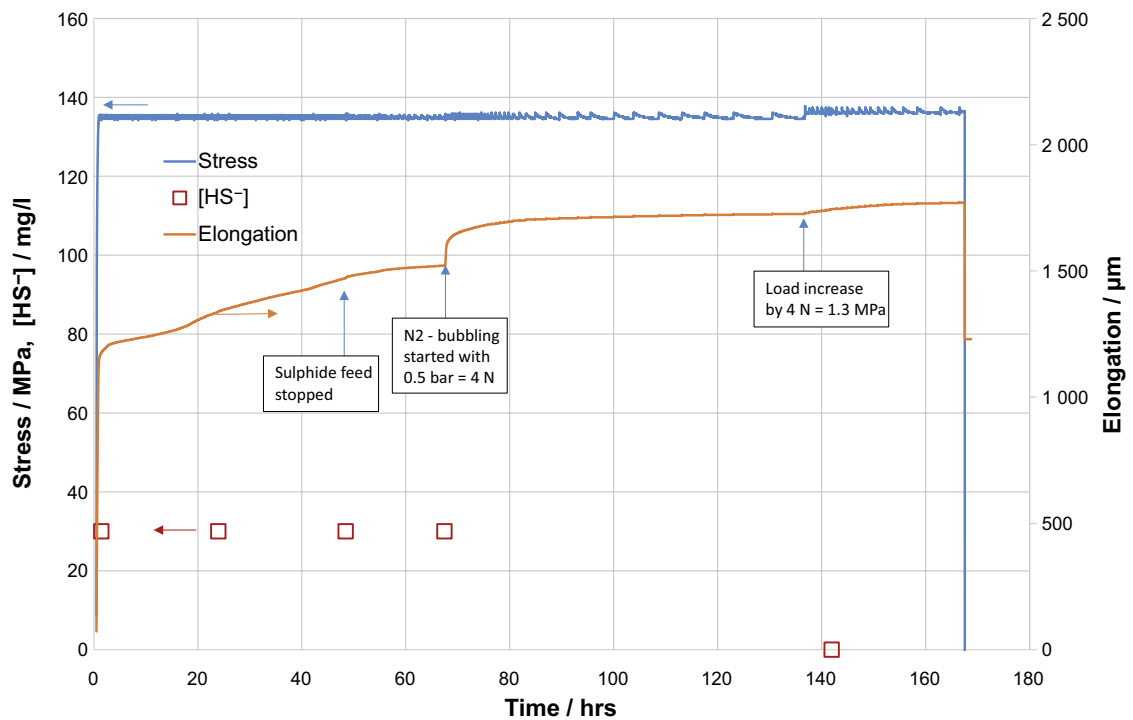


Figure 5-7. The stress and elongation and sulphide concentration as a function of time for sulphide test 1.

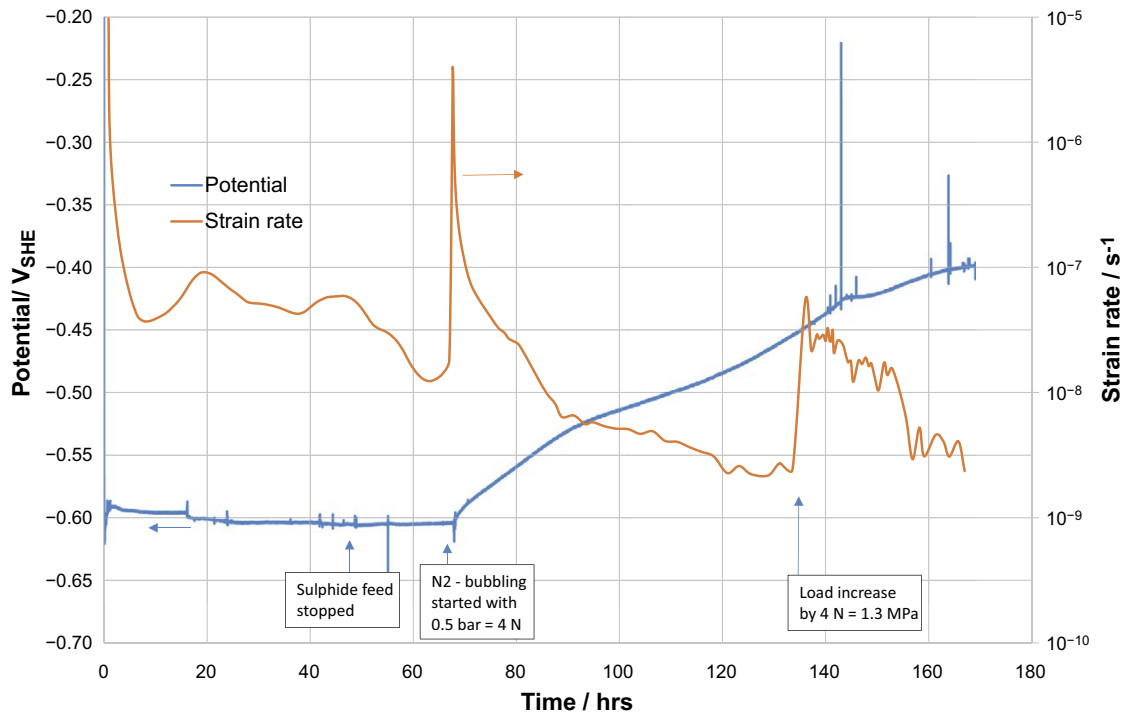


Figure 5-8. The corrosion potential and strain rate as a function of time for sulphide test 1.

Figure 5-9 shows the surface appearance of the creep specimen after sulphide test 1. The sulphide film has clearly exfoliated from most of the surface. This is due to the creep straining, since the coupon sample exposed in the same experiment did not show similar exfoliation of the sulphide film, Figure 5-10.



Figure 5-9. The surface appearance of the creep sample after sulphide test 1.



Figure 5-10. The surface appearance of the coupon sample (no straining) after sulphide test 1.

5.2.2 Sulphide test 2

The corrosion potential and the sulphide concentration are shown in Figure 5-11 as a function of time. Before starting the creep test, the sulphide concentration was measured from the outlet as 20 mg/l. After this, the inlet concentration was checked, and found to be at the expected level of 30 mg/l. After some trouble shooting a small leakage was found in one of the piping connections, and fixed. The troubleshooting period lasted for about 0.5 hrs, after which the outlet was checked again at about $t = 4$ hrs and found to be at the correct level. After this, the loading was initiated at about $t = 4$ hrs. The stress and elongation during the second sulphide test are shown in Figure 5-12 as a function of time. Also the sulphide measurement results are shown in the figure at appropriate times. Figure 5-13 shows the strain rate and corrosion potential as a function of time. After the initial period the corrosion potential and the strain rate remained rather stable during the exposure.

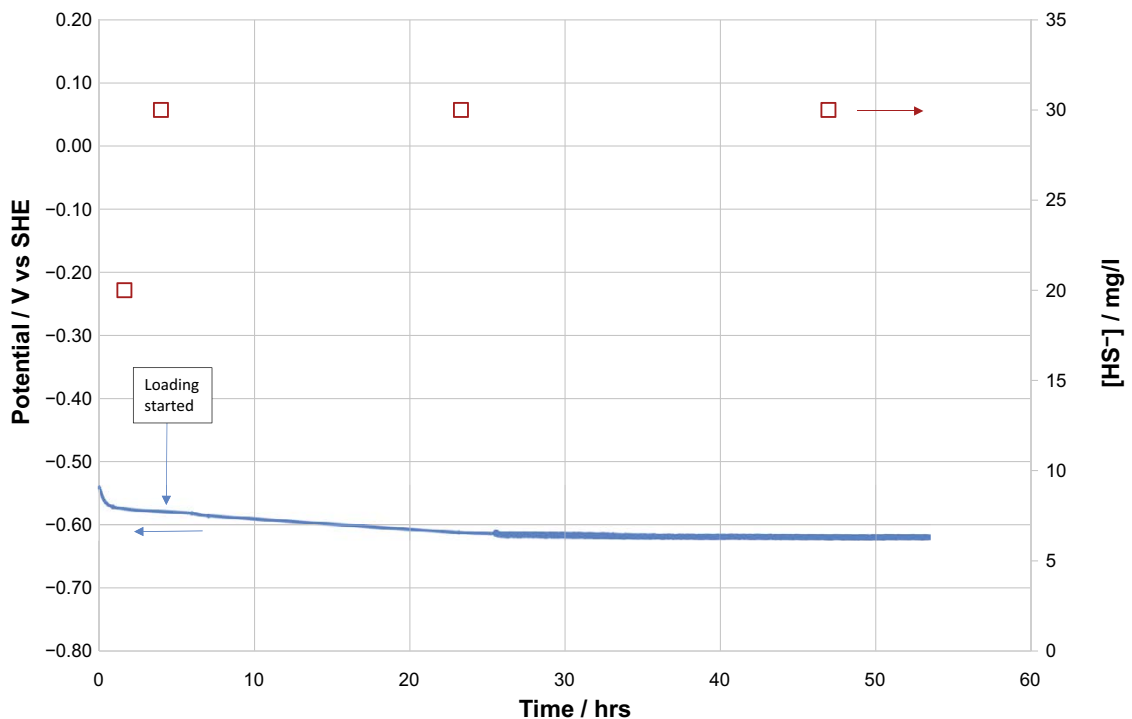


Figure 5-11. The corrosion potential and sulphide concentration as a function of time for sulphide test 2.

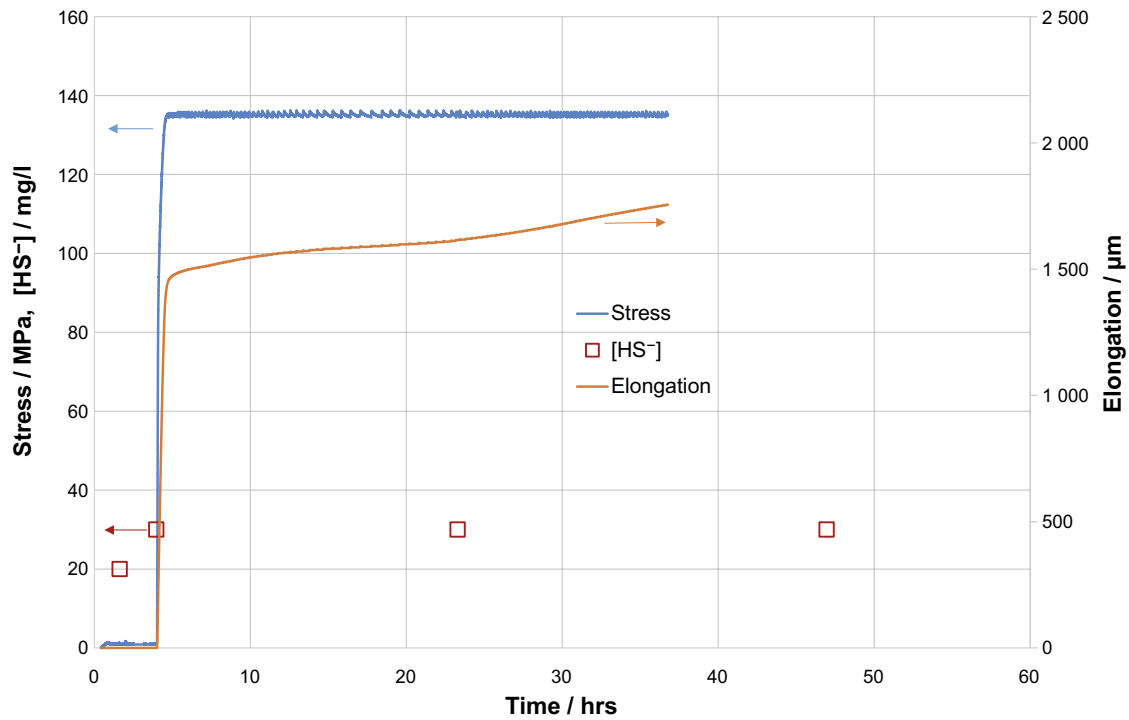


Figure 5-12. The stress and elongation as a function of time for sulphide test 2. The times of measurement and levels of sulphide measured are also indicated.

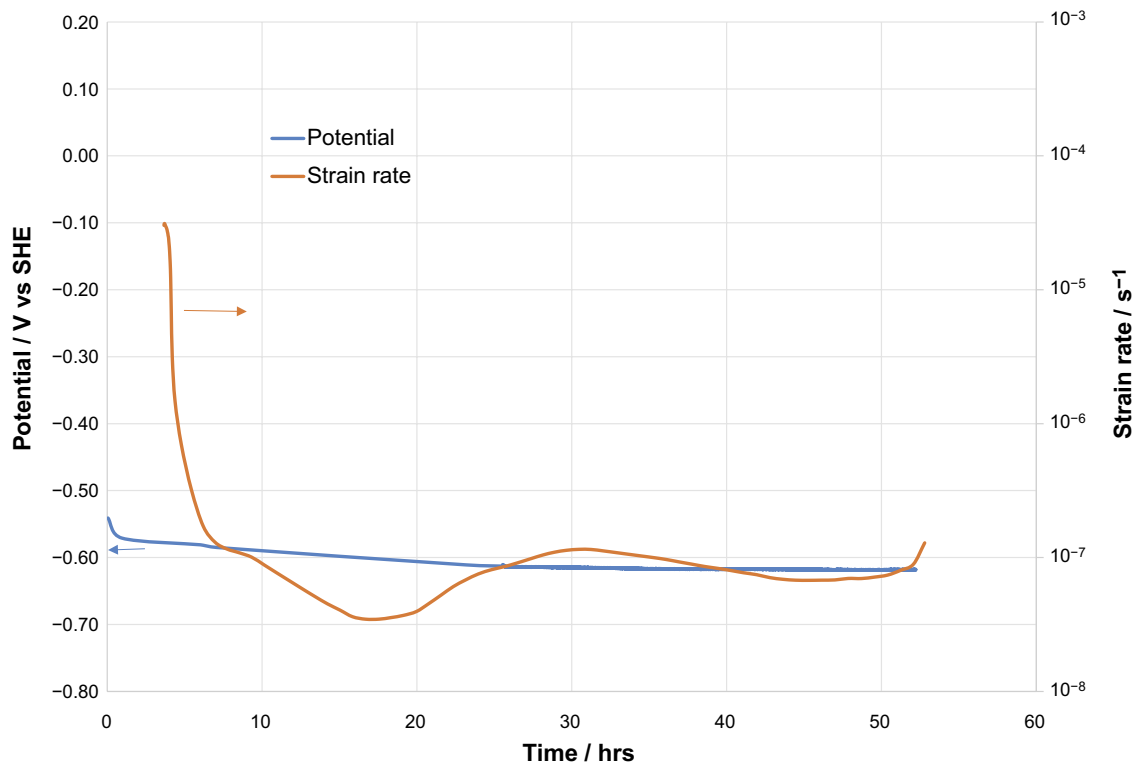


Figure 5-13. The corrosion potential and strain rate as a function of time for sulphide test 2.

The sample from sulphide test 2 was removed from the autoclave immediately after reaching 48 hrs of exposure and photographed by mobile phone camera (Figure 5-14a), since it was necessary to minimize the time between opening up the autoclave, preparing the HME-samples and placing them in a liquid nitrogen container. Roughly 2/3 of the body waist part was cut off, the sulphide film was

removed by SiC paper, after which the sample was cut in two roughly equal pieces. The two pieces were then rinsed with MilliQ water, further rinsed with ethanol, dried using a hair blower with a very gentle heat and then placed in a small paper bag. The paper bag was immediately placed in a liquid nitrogen container. The total time spent from opening up the autoclave until placing the samples in the liquid nitrogen container was about 23 minutes. The remaining piece of the specimen body was placed in a desiccator to be later examined with SEM. Two SEM samples were prepared, one for the surface investigation and one for cross-section studies.

Comparing Figure 5-9 and Figure 5-14 it is clear that while almost all of the surface film on the sample from sulphide test 1 had exfoliated, the surface film on the sample from sulphide test 2 had stayed mostly adhered to the base metal surface (only one area showed signs of exfoliation). Since the total permanent strain level in the two samples was about the same (about 4.7 % and 4.2 % for sulphide test 1 and 2, respectively), the exfoliation of the surface film during sulphide test 1 would not be expected to be related to the total strain level achieved.

Figure 5-15 shows the surface appearance of the coupon specimen exposed during the sulphide test 2, with no signs of surface film exfoliation.

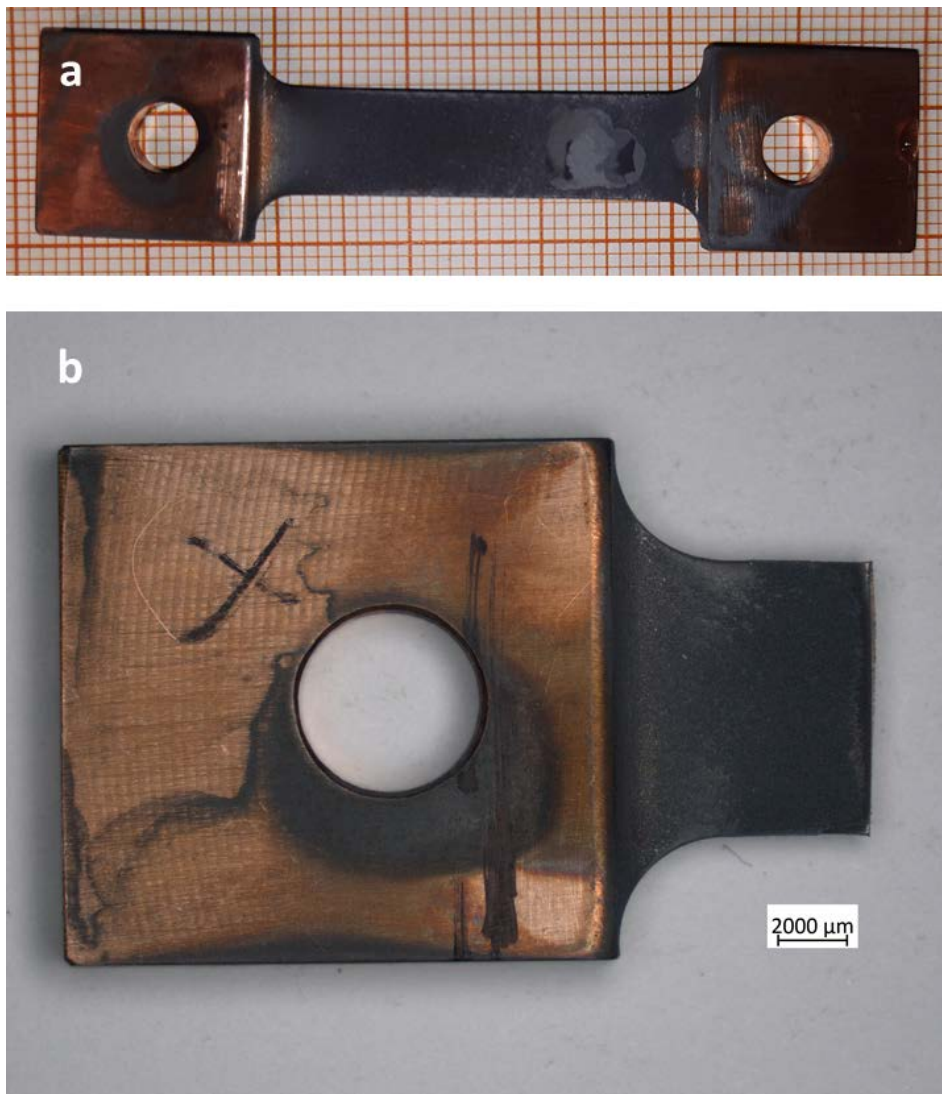


Figure 5-14. The surface appearance of the creep sample after sulphide test 2; a) photo by mobile phone camera and b) the remaining piece from which the SEM-samples were made (after cutting off the parts that went to hydrogen measurement).



Figure 5-15. The surface appearance of the coupon sample after sulphide test 2.

5.3 HME and SEM studies

5.3.1 Hydrogen measurement

Hot Melt Extraction (HME) technique with TC-detector was used to measure the hydrogen content in the two samples. The hydrogen concentrations were 5.86 and 6.19 ppm. The average hydrogen concentration measured earlier for the same material (four samples in as-received condition), (Huutilainen et al. 2022) was 3.24 ppm (in the range from 2.72 to 3.5 ppm). This indicates that during the exposure of Cu-OFP creep specimen (under constant loading) to sulphide containing environment, hydrogen does accumulate into the material.

5.3.2 SEM studies of the coupon samples

Two coupon samples were studied with SEM; one coupon from each sulphide exposure (the coupons were exposed in the same experiments as the creep specimens). Figure 5-16 shows the surface morphology of both coupon samples. The surface layer crystals in case of sulphide test 2 (in which at the end of the 48 hr exposure the sample was immediately removed from the sulphide containing water), Figure 5-16a and b, are well defined and somewhat larger in comparison to the crystals in case of sulphide test 1 (in which the sample stayed in water for about 100 hrs after the sulphide was removed). The surface morphology indicates (rounded edges of the surface crystals in sulphide test 1) that after removal of sulphide from the water, the copper sulphide crystals have a tendency to dissolve. In addition, as shown in Table 5-1 (see Section 5.3.4), the total film thickness in case of both coupon and creep samples was lower (by a factor of about 2) for sulphide test 1, in comparison to sulphide test 2, despite of the much longer exposure time in case of sulphide test 1. However, no marked difference was found in the chemical composition of the surface layers (outer layer) in the two sulphide tests, Figure 5-17. It is noteworthy here that O was found in both sulphide test 1 and 2, with somewhat higher concentration in the surface layer on the sample from sulphide test 1. More than half of the spots showed some Ni, the obvious source of which is dissolution from the autoclave walls.

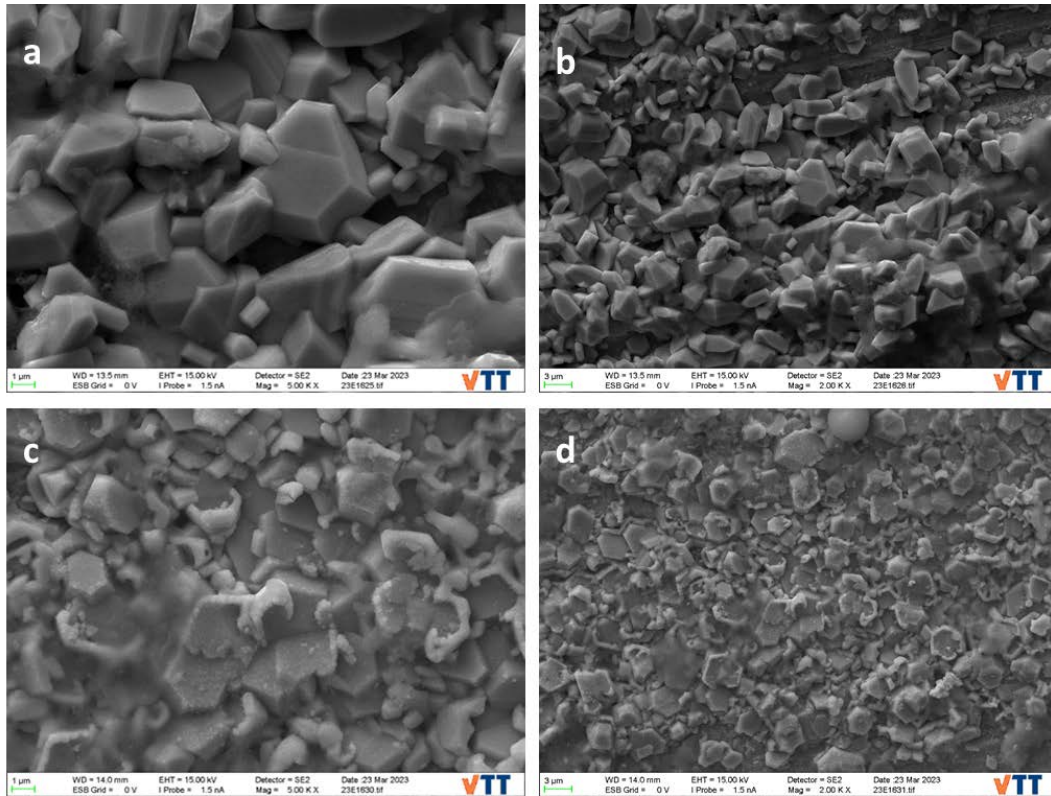
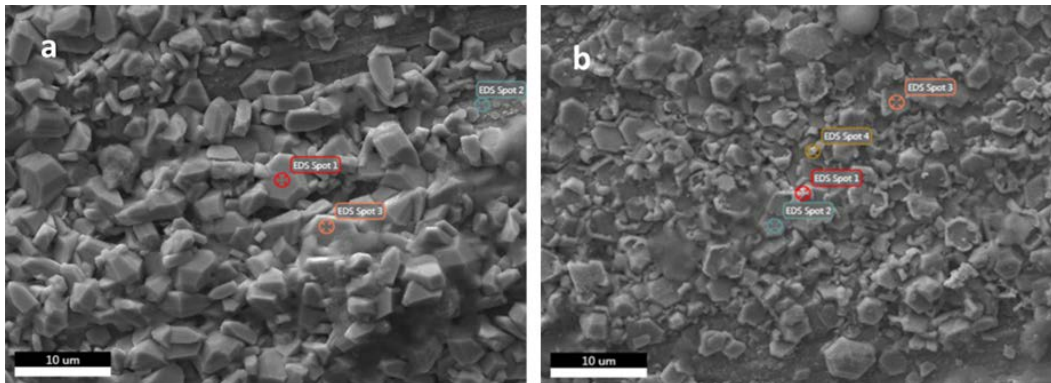


Figure 5-16. Surface morphology of the coupon samples from sulphide test 2 (a and b) and sulphide test 1 (c and d).



	Spot 1	Spot 2	Spot 3
Element			
O	5.84	16.71	5.67
Na	0.00	0.00	0.00
Si	0.00	0.00	0.00
P	0.00	0.92	0.00
S	30.22	3.04	30.08
Ni	3.88	5.34	3.69
Cu	60.05	73.98	60.56

	Spot 1	Spot 2	Spot 3	Spot 4
Element				
O	17.07	3.60	8.82	11.45
Na	0.00	4.52	0.00	0.00
Si	0.21	0.47	0.00	0.00
P	0.00	0.09	0.00	0.00
S	27.60	20.88	29.81	28.05
Ni	2.75	0.00	4.43	3.50
Cu	52.41	70.44	56.94	57.00

Figure 5-17. SEM-EDX analyses of the coupon samples from sulphide test 2 (a) and sulphide test 1 (b). Concentrations in atomic %, normalized to 100 % after the contribution of carbon has been removed from the data.

The surface films on the coupon specimens revealed a double-layer structure, i.e. an outer layer and an inner layer, Figure 5-18. The thickness of the inner layer on sulphide test 1 and sulphide test 2 coupon specimens was 0.9 μm and 1.1 μm , whereas the total thicknesses were 2.2 μm and 4.8 μm , respectively. In the cases where the contribution of carbon (from the SEM-sample preparation) was not insignificant, the concentrations of elements other than carbon were normalized to 100 % (excluding carbon). The EDX-map in Figure 5-19 shows that both surface film layers in case of sulphide test 2 consist of Cu and S (with a small amount of Na originating in the buffer solution, and a very small amount of P), rather evenly distributed within the two layers. It is surprising that no O was found, although the corresponding surface sample showed about 5.8 a% of O. The film on the sample from sulphide test 1 had an almost identical composition, with only a small percentage of O. However, the EDX-map in case of sulphide test 1, Figure 5-20, shows a thin but clear O and Cu enriched layer at the interface between the inner layer and the matrix (the O and Cu enriched layer is discernible also in the BSE picture, Figure 5-18d). The thickness of the O and Cu enriched layer is over 100 nm, and can thus not be a remnant of the airborne oxide, the thickness of which is only a few nm.

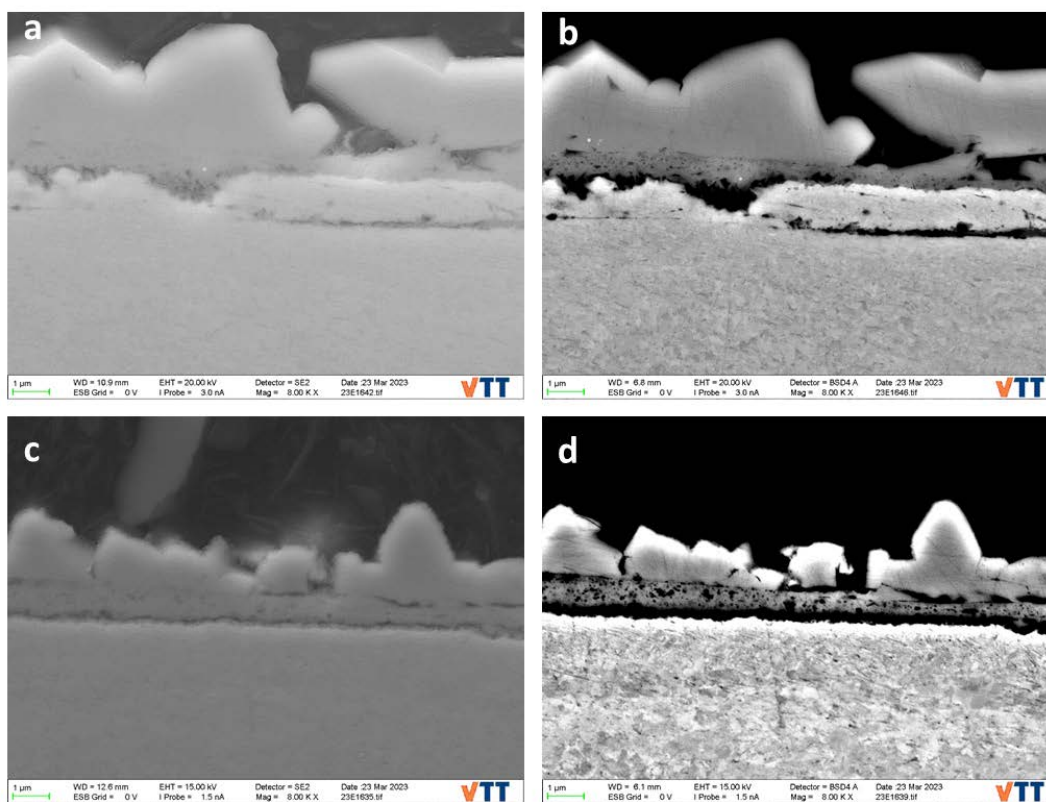


Figure 5-18. Cross-sections of the coupon samples from sulphide test 2 (a and b) and sulphide test 1 (c and d). Left = SE and right = BSE mode.

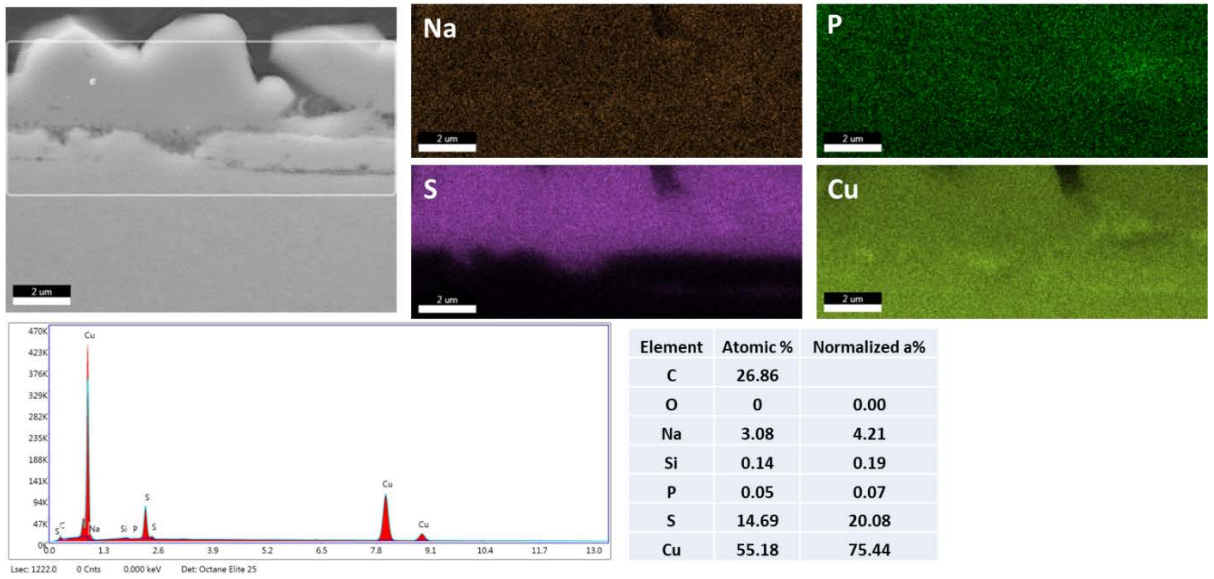


Figure 5-19. SEM-EDX analyses of the coupon sample from sulphide test 2.

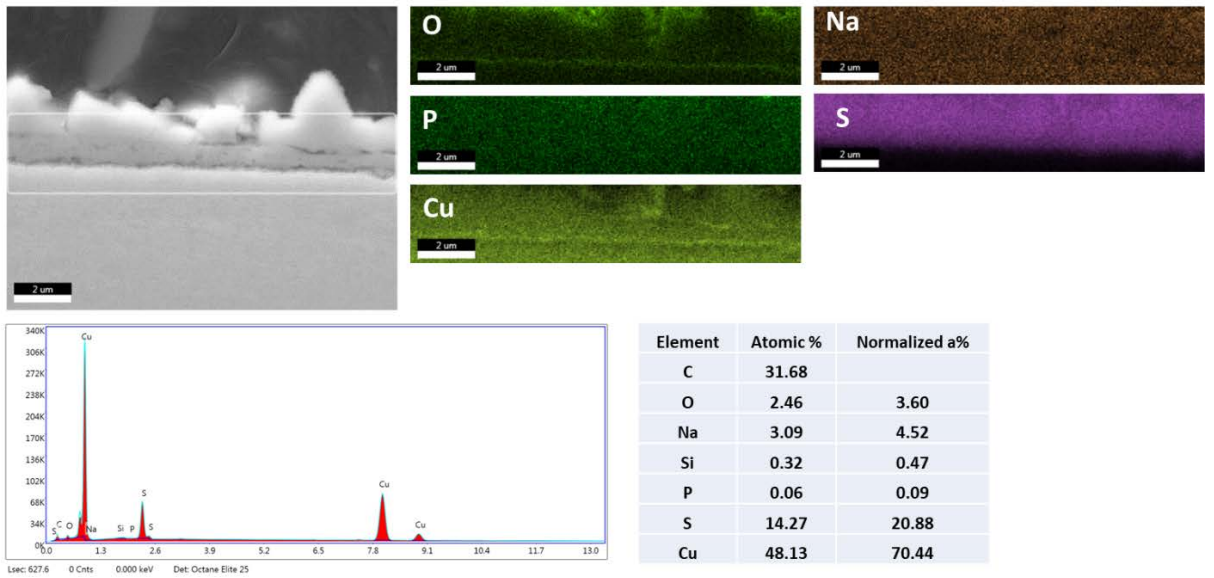


Figure 5-20. SEM-EDX analyses of the coupon sample from sulphide test 1.

5.3.3 SEM studies of the creep specimens

The morphology of the surface film on the creep specimens is shown in Figure 5-21. When comparing with the surface films on the coupon specimens, Figure 5-16, the surface film can be described as nano-crystalline. The EDX analyses of the creep specimen from sulphide test 2, Figure 5-22a, showed a clearly smaller amount of S in the surface film present in areas from where the thick sulphide film had exfoliated than in the corresponding coupon sample, about 17 a% and 30 a%, respectively. The difference in sulphur concentration may be related to the presence of only a single layer of sulphide film on the creep specimen, i.e. a lower concentration of sulphur in the film indicates a lower surface concentration of sulphur in the vicinity of the film on the water side, and therefore less probability for supersaturation and resulting deposition of the outer layer crystals. Hypothetically, this can be explained by the dynamic creep strain constantly revealing new fresh surface which rapidly gets sulphidized and thereby prevents supersaturation nearby the surface, since the rate of sulphide film formation and overall Cu-OFP corrosion in sulphide environment is supposed to be mass transfer limited. Another way of looking into this finding is the nano-crystalline film forming on highly energetically favourable new nucleation points being exposed due to creep strain, thus effectively consuming the nearby HS^- -ions and preventing supersaturation necessary for the deposition of the outer layer crystals. These considerations would also explain the much smaller average crystal size in the case of the creep specimens.

The sulphide film on the creep specimen from sulphide test 1 had mostly exfoliated, Figure 5-9, whereas that from sulphide test 2, Figure 5-14, showed an almost intact appearance. This indicates that exfoliation occurred only after removing sulphide from the water. The other possibility is that exfoliation occurred on both specimens, and the surface film on the specimen in sulphide test 2 was quickly repaired by the sulphide present in the water. This possibility is, however, unlikely, since the exfoliation occurs as rather thick and large pieces of the surface film, which would be expected to leave a noticeable “footprint” on the surface, even if further sulphide film formation would occur.

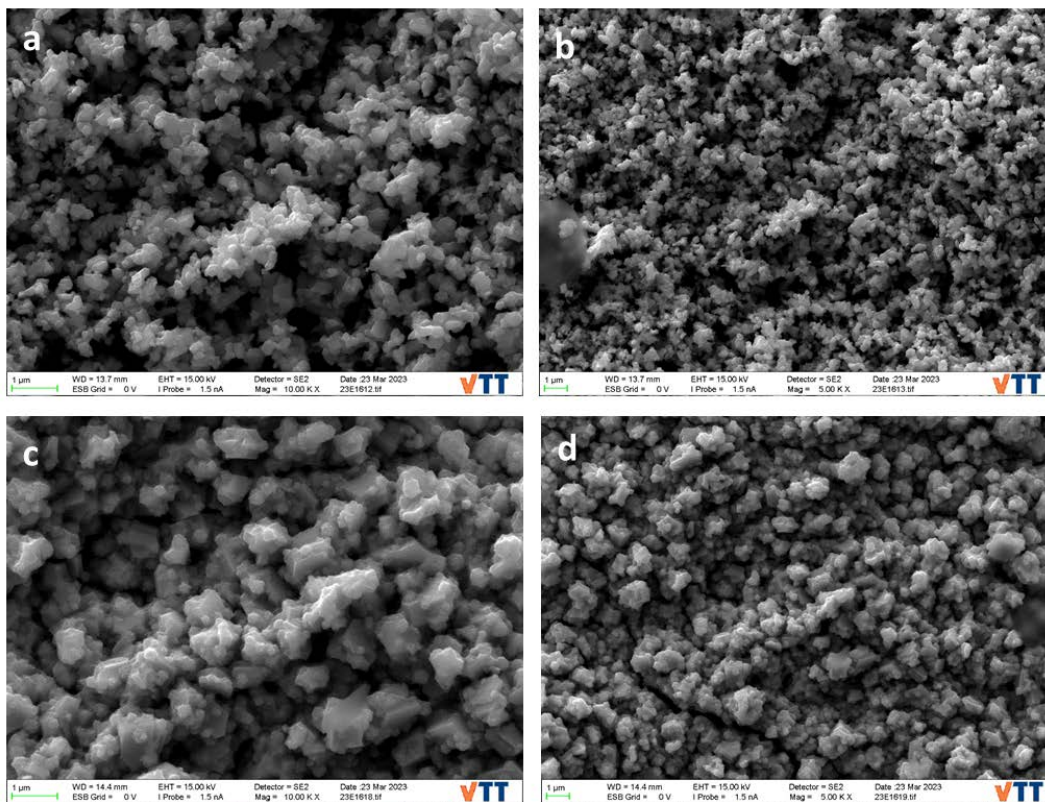
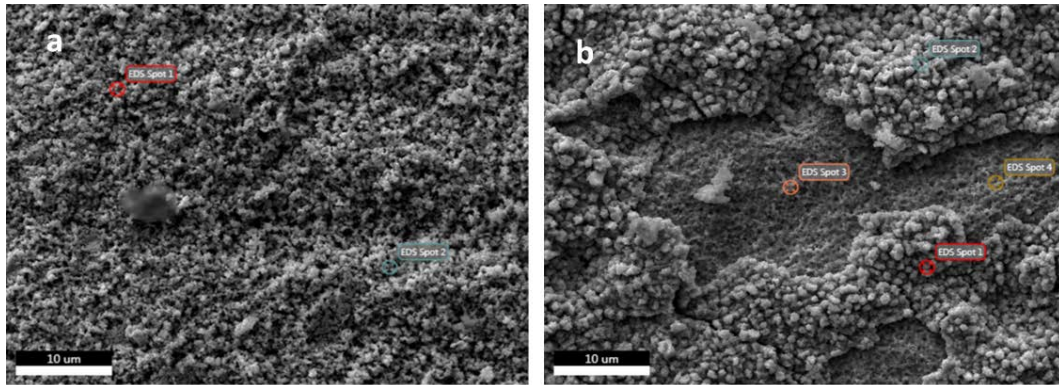


Figure 5-21. Surface morphology of the creep samples from sulphide test 2 (a and b) and sulphide test 1 (c and d).

Figure 5-22b shows EDX analyses from two areas on the creep specimen from sulphide test 1, one with the (nano-crystalline) sulphide film (EDX spots 1 and 2) and one from which the sulphide film has exfoliated (EDX spots 3 and 4). The sulphide film (EDX spots 1 and 2) showed a composition rather close to that on the corresponding coupon sample (Figure 5-17), while the area from which the sulphide film had exfoliated (EDX spots 3 and 4), showed basically only Cu (with a small amount of Ni). The total surface area of fully exfoliated regions like that shown in Figure 5-22b was still smaller than those that showed a nano-crystalline outer film.



	Spot 1	Spot 2
Element		
O	5.34	1.01
Na	0.00	0.00
Si	0.00	0.00
P	0.00	0.00
S	16.60	18.60
Ni	4.50	2.64
Cu	73.57	77.76

	Spot 1	Spot 2	Spot 3	Spot 4
Element				
O	10.33	8.63	8.36	5.32
Na	0.00	0.00	0.00	0.00
Si	0.00	0.00	0.00	0.00
P	0.00	0.00	0.00	0.00
S	28.34	25.67	1.29	0.00
Ni	0.00	0.00	0.00	5.28
Cu	57.78	62.68	84.91	89.40

Figure 5-22. SEM-EDX analyses of the creep sample from a) sulphide test 2 and b) sulphide test 1. Concentrations in atomic %, normalized to 100% after the contribution of carbon has been removed from the data where necessary.

As shown in Figure 5-23, the surface film on both of the creep samples had a single-layer structure, with much more porosity than in the corresponding coupon samples (see Figure 5-18). The thickness of the film formed on the creep specimen from sulphide test 1 and 2 was 2 μm and 6 μm , respectively. The EDX-map in Figure 5-24 shows that the surface film layer in case of sulphide test 2 consists of Cu and S (with a small amount of Na and O, and a very small amount of Si and P). On the other hand, the EDX-map in case of sulphide test 1, Figure 5-25, shows almost four times higher concentration of O and somewhat lower concentration of Cu and S, as well as a thin Cu and O enriched layer at the interface between the inner layer, similar to but not nearly as clear as that found in the corresponding coupon sample, Figure 5-20. The coupon sample from sulphide test 2 did not show such O and Cu enriched layer, Figure 5-19, while the creep sample from the sulphide test 2 showed a possible, very weak, O and Cu enriched layer, Figure 5-24. Thus it seems that the appearance of the O and Cu enriched layer is favoured by the sample being under continuous straining and by the sample being exposed to a sulphide free water after initial exposure to a HS^- containing water. The layer could thus be related to the dissolution of the existing sulphide film, accelerated by the continuous straining.

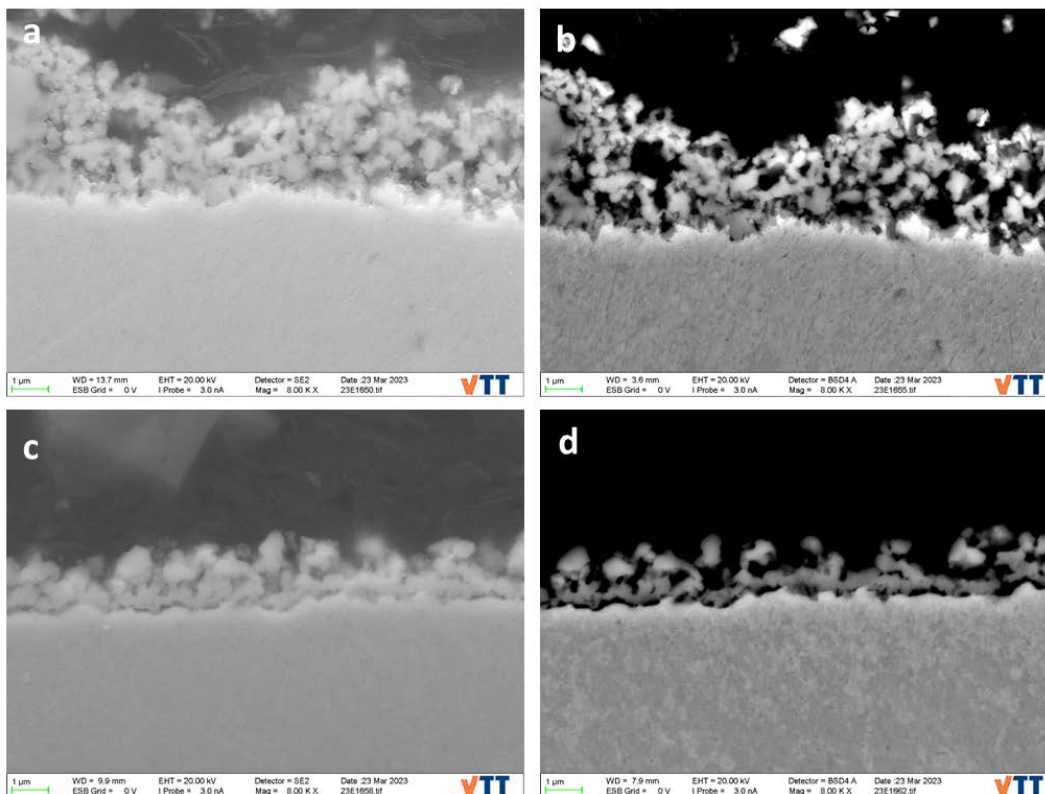


Figure 5-23. Cross-sections of the creep samples from sulphide test 2 (a and b) and sulphide test 1 (c and d). Left = SE and right = BSE mode.

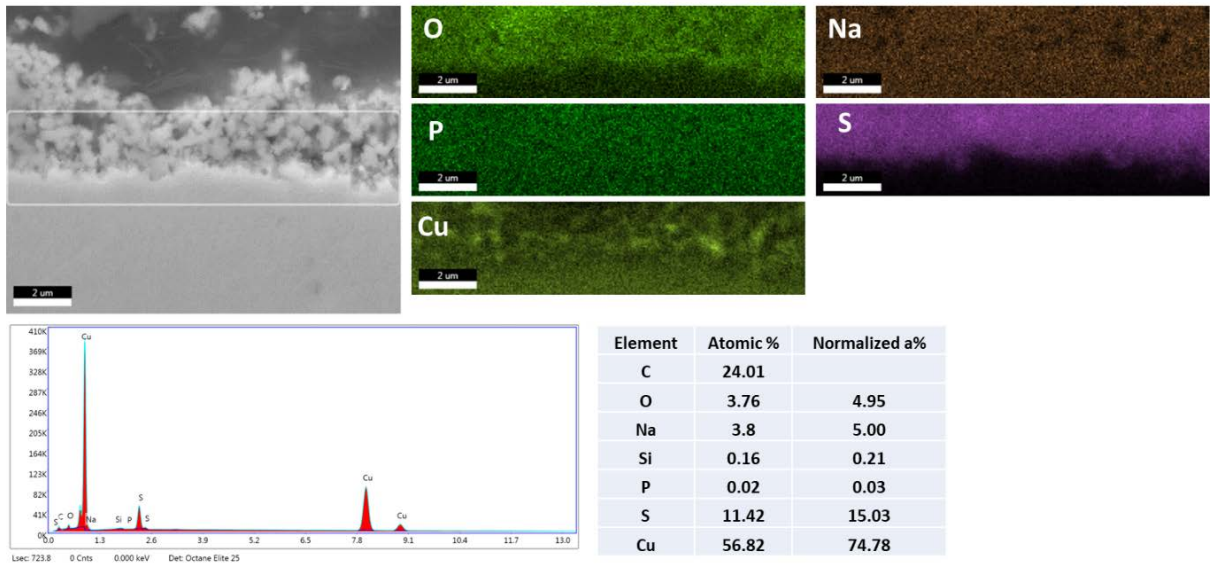


Figure 5-24. SEM-EDX analyses of the creep sample from sulphide test 2.

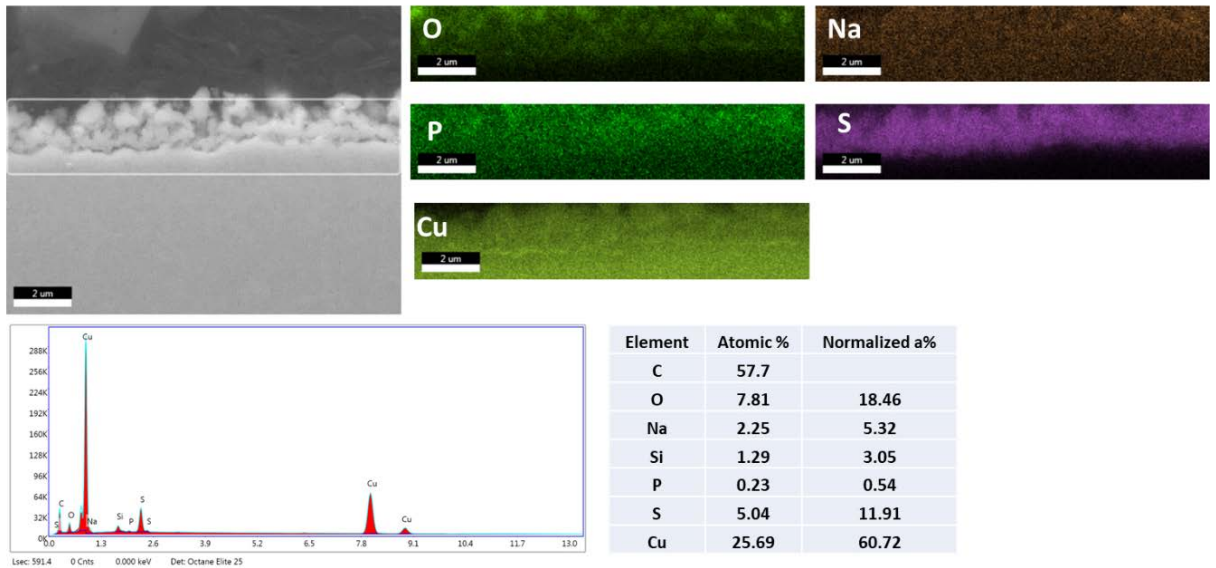


Figure 5-25. SEM-EDX analyses of the creep sample from sulphide test 1.

5.3.4 Compilation of data from SEM studies

In order to ease the comparison of results from different SEM-studies, the data on film thicknesses is gathered in Table 5-1 and the SEM-EDX point analyses data in Table 5-2.

From Table 5-1, the total film thickness in case of sulphide test 1 is about a factor of 2 smaller than that in sulphide test 2, despite the exposure time in sulphide test 1 was much longer. Thus, the removal of sulphide from the water (and gas) phase in the autoclave in sulphide test 1 has resulted in some dissolution of the sulphide film. It is also noteworthy that the films on creep samples showed only a single layer of surface film, whereas the coupon samples showed the normal double layer structure.

Table 5-1. Film thicknesses (in μm) as measured from SEM cross-sections as 14 point average.

Sample	Total	Inner film	Outer film
Sulphide 1 coupon	2.2	0.9	1.3
Sulphide 1 creep	1.5	-	-
Sulphide 2 coupon	4.8	1.1	3.7
Sulphide 2 creep	3.5	-	-

Table 5-2. SEM-EDX point analyses data (normalized a%).

Sulphide 1 coupon					Sulphide 2 coupon			
	Spot 1	Spot 2	Spot 3	Spot 4		Spot 1	Spot 2	Spot 3
Element					Element			
O	17.07	3.60	8.82	11.45	O	5.84	16.71	5.67
Na	0.00	4.52	0.00	0.00	Na	0.00	0.00	0.00
Si	0.21	0.47	0.00	0.00	Si	0.00	0.00	0.00
P	0.00	0.09	0.00	0.00	P	0.00	0.92	0.00
S	27.60	20.88	29.81	28.05	S	30.22	3.04	30.08
Ni	2.75	0.00	4.43	3.50	Ni	3.88	5.34	3.69
Cu	52.41	70.44	56.94	57.00	Cu	60.05	73.98	60.56

Sulphide 1 creep					Sulphide 2 creep		
	Spot 1	Spot 2	Spot 3	Spot 4		Spot 1	Spot 2
Element					Element		
O	10.33	8.63	8.36	5.32	O	5.34	1.01
Na	0.00	0.00	0.00	0.00	Na	0.00	0.00
Si	0.00	0.00	0.00	0.00	Si	0.00	0.00
P	0.00	0.00	0.00	0.00	P	0.00	0.00
S	28.34	25.67	1.29	0.00	S	16.60	18.60
Ni	0.00	0.00	0.00	5.28	Ni	4.50	2.64
Cu	57.78	62.68	84.91	89.40	Cu	73.57	77.76

6 Discussion and Conclusions

The transient increase in creep rate of Cu-OFP in water, due to removal of sulphide from the water, as reported earlier (Ikäläinen et al. 2022), was in this work shown to be a repeatable phenomenon. As evidenced by the data shown in Figure 5-8, the increase in the creep rate is very rapid, the most intense increase taking place within minutes from starting to purge the gas phase in the autoclave with N₂.

The high rate of the process is rather surprising, taking into account that as the H₂S in the gas phase is removed by N₂ bubbling, the sulphide ion (HS⁻) in the water phase needs to first react with H⁺ to form more gaseous H₂S (trying to reach a new equilibrium with the gas phase). In order for this reaction to influence the surface film or the hydrogen concentration inside the Cu-OFP material, still further processes are required.

Hydrogen charging via cathodic polarization in highly acidic environment with added recombination poison causes increase in the strain rate of Cu-OFP, see e.g. Yagodzinsky et al. (2012). Although exposure to sulphide containing near neutral water is by no means equal to cathodic charging in terms of loading hydrogen into the material, increase in hydrogen concentration during the first 48 hrs of sulphide exposure was confirmed by measurements (HME) in this work. From earlier work (Ikäläinen et al. 2022) it is known that the hydrogen loading (at this rate) does not, however, result in an elevated creep rate. Hypothesizing that all the accumulated hydrogen did come out in the latter part of that test, within 30 min, we would be looking into a filling up period of 64 hrs and coming out period of 0.5 hrs. The ratio (64/0.5) is about 130, which is about the factor of increase in the creep rate observed. In this line of hypothetical thinking, the effect of flux in and out (the mechanism) remains the same, whereas the magnitude of the flux out in the present case would be over 100 times higher. In previous work (Ikäläinen et al. 2022) cathodic charging tests in near neutral pH buffer solution were inconclusive in that an increase of strain rate was observed as a result of the first three cathodic polarisation periods, but not after that in the following four cathodic polarisations.

The corrosion potential measured for Cu-OFP in the present case (pH = 7.2, [HS⁻] = 30 mg/l), $E_{oc} \approx -0.6 V_{SHE}$, corresponds to the Cu₂S/Cu-equilibrium potential (Metso Outotec 2007), and lies about 0.2 V below the so-called hydrogen line ($E_{eq}(H^+/H_2)$), below which water starts to decompose producing hydrogen. As shown in Figure 5-8, the corrosion potential of Cu-OFP starts to increase when the N₂ bubbling is initiated. However, the rate of increase in the corrosion potential is only about 3 mV/hr, indicating that no major changes in the surface film stability and/or composition would be expected to take place within at least the first 10 to 20 hrs after the start of the N₂ bubbling. Actually, the corrosion potential remained in the stability area of Cu₂S during the whole remaining exposure time, even after all sulphide had been removed from the water.

Sulphide exposure was found to increase the hydrogen concentration in Cu-OFP, by about a factor of two. It is worth noting here that the reference value of hydrogen concentration measured for the Cu-OFP material used in this study, 3.24 ppm, is already very high in comparison with the normally found level of about 0.5 ppm, and the value reported by the material supplier of the Cu-OFP material used in this study (0.43 ppm, Table 3-2).

However, since the reference value reported earlier is an average of four measurements (Huotilainen et al. 2022), and since the earlier reported data (Huotilainen et al. 2022) as well as the present measurements were performed with the same equipment using the same procedures, and since the increase on top of the reference value in hydrogen concentration found in the present work was about 3 ppm, it is clear that the hydrogen concentration of Cu-OFP creep sample was markedly increased due to the sulphide exposure.

The SEM-studies showed that the sulphide film forming on coupon samples in both exposures had a double-layer structure with the crystal size in the outer layer in the µm range, whereas the surface film on the creep samples was a monolayer, with crystal size in the range of 0.1 µm and below. The surface film thickness was clearly less for the samples with continuing exposure after removal of sulphide from the water, and the outer layer crystals on the coupon sample showed a morphology, rounding of the edges, indicating some dissolution. Thus, sulphide removal did result in some dissolution of the surface film, although exfoliation was also clearly influencing the thickness of the samples in sulphide test 1.

The finding of a layer enriched in Cu and O at the metal/film interface on both the coupon and creep specimens in sulphide test 1 indicates that the sulphide film in both cases is porous and not protective, since oxygen containing ions have been able to diffuse/migrate through the existing sulphide film. Formation of such a layer could be the reason for the exfoliation of the sulphide film, although, since exfoliation was not seen on the coupon specimen, the slow deformation in the creep specimen plays an important role in the exfoliation process.

As an additional finding, micro-cracks were found to open up on the Cu-OFP tensile specimen surface tested to fracture in air. The micro-cracks are due to pre-existing defects/weak grain boundaries within the material.

Based on the above findings, the following conclusions were made:

- hydrogen does enter Cu-OFP during exposure to sulphide containing water,
- the increase in Cu-OFP creep rate caused by removal of sulphide from the water occurs at such a high rate, that the mechanism is most likely that of hydrogen in the Cu-OFP moving out and causing excessive dislocation movement,
- dynamic creep deformation influences the morphology of the surface film forming on Cu-OFP; instead of the typical double-layer surface film, a single layer of nano-crystalline film is formed,
- straining of Cu-OFP tensile specimens to fracture causes micro-cracks to appear on the surface, originating from pre-existing defects.

References

SKB's (Svensk Kärnbränslehantering AB) publications can be found at www.skb.com/publications. SKBdoc documents will be submitted upon request to document@skb.se.

Huotilainen C, Hytönen N, Saario T, 2022. Hydrogen in Cu-OFP. VTT Research Report VTT-R-00048-22. SKBdoc 1977155 ver 1.0, Svensk Kärnbränslehantering AB.

Lilja C, 2021. Calculated by the Spana software of KTH. Stockholm: Kungliga Tekniska högskolan.

Ikäläinen T, Saario T, Que Z, 2022. Creep rate in Cu-OFP under applied electrochemical potential and presence of sulphide. SKB TR-22-05, Svensk Kärnbränslehantering AB.

Metso Outotec, 2007. HSC Chemistry-software Trelleborg: Metso Outotec.

Välimäki T, 2009. SKB T58 tube structure evaluation. Luvata Pori Oy Report 1.6.2009. SKBdoc 1216615 ver 2.0, Svensk Kärnbränslehantering AB.

Yagodzinsky Y, Malitckii E, Saukkonen T, Hänninen H, 2012. Hydrogen-enhanced creep and cracking of oxygen-free phosphorus-doped copper. Scripta Materialia 67, 931–934.

SKB is responsible for managing spent nuclear fuel and radioactive waste produced by the Swedish nuclear power plants such that man and the environment are protected in the near and distant future.

[skb.se](https://www.skb.se)